ICENES2007 13th International Conference on Emerging Nuclear Energy Systems
3-8 July 2007, İSTANBUL, TURKEY

TRANSMUTATION OF HIGH LEVEL WASTES IN A FUSION-DRIVEN TRANSMUTER (FDT)

Nesrin DEMİR*, Gamze GENÇ, Hüseyin YAPICI
* Erciyes University, Faculty of Engineering, Department of Mechanical Engineering
nkayatas@erciyes.edu.tr

ABSTRACT

This study presents the transmutations of both the minor actinides (MAs: ^{237}Np, ^{241}Am, ^{243}Am and ^{244}Cm) and the long-lived fission products (LLFPs: ^{99}Tc, ^{129}I and ^{135}Cs), discharged from high burn-up PWR-MOX spent fuel, in a fusion-driven transmuter (FDT) and the effects of the MA and LLFP volume fractions on their transmutations. The blanket configuration of the FDT is improved by analyzing various sample blanket design combinations with different radial thicknesses. Two different transmutation zones (TZ_{MA} and TZ_{FP} contain the MA and LLFP nuclides, respectively) are located separately from each other. The volume fraction of the MA (VF_{MA}) is raised from 10 to 20% stepped by 2%. The MAs are cladded with the graphite (10%) and cooled with the high-pressured helium gas to transfer the nuclear heat. The volume fraction of helium is reduced from 80 to 70% depending on that of MA. Furthermore, the volume fraction of graphite is raised from 10 to 80% stepped by 5% to slow down the energy of neutrons entering into the TZ_{FP} while the volume fraction of LLFP (VF_{FP}) is reduced from 80 to 10% depending on the graphite volume fraction. The calculations are performed for an operation period (OP) of up to 10 years by 75% plant factor (η) under a neutron wall load (P) of 5 MW/m^2 to estimate neutronic parameters and transmutation characteristics per D-T fusion neutron. The transmutation fractions of LLFPs decrease quasi-linearly with the increase of VF_{FP} and these values increase with the increase of VF_{MA}. The ^{99}Tc among the LLFP nuclides has the highest transmutation fraction.

Keywords: Fusion reactors; Fusion-driven transmuters; Minor actinides; Long-lived fission products; Tritium breeding.

1. INTRODUCTION

One of the most important problems that must be solved in nuclear technology is how to destroy nuclear wastes, either generated in the form of spent fuel discharged from conventional reactors or in the form of high level waste (HLW) originating from extracting plutonium from spent fuel in a safe manner with respect to public health and the environment. Two types of potential nuclear waste can be distinguished: (1) long-lived fission products (LLFPs: ^{129}I, ^{99}Tc, ^{135}Cs, etc.) and (2) transuranium (TRU) elements (those beyond uranium on the periodic table), which mainly include plutonium isotopes and minor actinides (MAs: isotopes of Np, Am and Cm). The MAs can only be destroyed by fissioning or transforming them into easily fissionable nuclei by a neutron capture process. The LLFPs, unlike the MAs, cannot be destroyed by fission in a reasonable neutron field. They would be transmuted into stable or short-lived radioactive species by means of capture reactions. The transmutation of LLFPs, in contrary to the transmutation of TRUs, is, therefore, a purely neutron consuming process and requires excess of neutrons.

Transmutation can be defined as the transformation of one isotope into another isotope by changing its nuclear structure. Two examples of nuclear transmutation from exposure of isotopes to neutrons are neutron-induced fission and neutron capture. In order to transmute efficiently the HLW, the high intensity neutron source is needed. High energetic neutrons released from fusion reactions enter into a sub-critical blanket containing the plutonium isotopes, the MAs and/or the LLFPs to transmute these nuclides either through fission or neutron capture reactions followed by decay. Hence, transmutation of the HLW utilizing deuterium-tritium, D-T, fusion neutrons is a good choice for an early application of fusion. The fusion-driven transmutation concept will lead to improved pathways to fusion power as well as make competitive applications available earlier than the power application of fusion energy. Based on this concept, many research groups have investigated the HLW transmutation potential of various FDTs. According to the kind of HLW considered in these studies, the investigations would be categorized in three groups: the transmutations of (1) only MAs [1-7], (2) only LLFPs [8-12] and (3) both MAs and LLFPs [13-19]. Most of them have attempted to use the fast neutron for burning and/or transmutation (B/T) of MAs, because the fission-to-capture ratios, σ_f/σ_c, of MAs are generally higher in fast region than those in thermal region. Nonetheless, they become highly fissionable under the high energetic fusion neutron environment.

In our recent works [20-26], comprehensive analyses on the MA transmutation capabilities of PROMETHEUS fusion reactor, force-free helical reactor (FFHR) and fusion-driven transmuter have been performed. These investigations have brought out that all of the reactors have a good MA transmutation potential.

2. BLANKET GEOMETRY

2.1. Fusion-Driven Transmuter Blanket Concept

The neutron leakage from the blanket can be thermalized and utilized for transmuting the LLFPs. The blanket surrounding the fusion plasma is one of the most important parts of a FDT, and generally, it contains four different zones: (1) first wall (FW) (plasma facing component zone); (2) tritium breeding zone (TBZ) including solid/liquid tritium breeding materials; (3) transmutation zone (TZ) containing the HLW; and (4) reflector zone (RZ) made of materials having high scatter cross-section.

In this study, for transmutation, the discharged MA (^{237}Np, ^{241}Am, ^{243}Am and ^{244}Cm) and LLFP (^{99}Tc, ^{129}I and ^{135}Cs) nuclides from high burn-up (50 GWd/tHM) PWR-MOX spent fuel represented as MOX22 in ref. [27] are used as the HLW. The isotopic fractions and densities of these nuclides are given in Table 1.

Table 1. Isotopic fractions and densities of MA and LLFP nuclides discharged from PWR-MOX spent fuel (50 GWd/tHM burn-up and 7 years cooling) [27]

MA				LLFP		
^{237}Np	^{241}Am	^{243}Am	^{244}Cm	^{99}Tc	^{129}I	^{135}Cs
4.30^{a}	58.28	26.05	11.28	0.39	0.1	0.51
20.25*	13.67	13.67	13.51	11.50	7.31	1.87

^{a} Isotopic fraction as percentage, * Density in g/cm^3

In order to accomplish the effective transmutation of both the MAs and the LLFPs, the FDT blanket has been improved by examining various configurations and so the improved blanket is plotted in Figure 1.

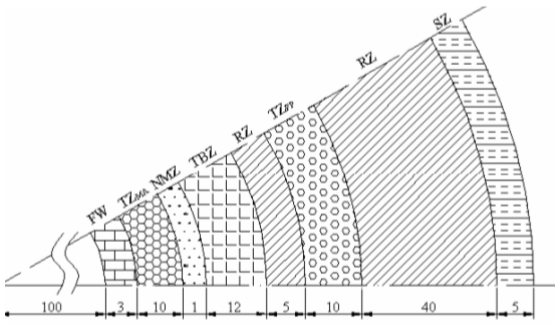

Figure 1. The improved blanket, (δ: radial thickness, FW: first wall, TZ_{MA}: MA transmutation zone, NMZ: neutron multiplier zone, TBZ: tritium breeding zone, RZ: reflector zone, TZ_{FP}: LLFP transmutation zone, and SZ: shielding zone), (the dimensions are given in cm and not in scale).

As is apparent from this figure, the blanket has eight zones consisting of seven different zones. The VF_{MA} is raised from 10 to 20% stepped by 2% to determine its effect on the transmutations of the MAs and the LLFPs while the volume fraction of coolant is reduced from 80 to 70% depending on the VF_{MA}. Nonetheless, it is adjusted carefully in order to keep the neutron multiplication coefficient (k_{eff})<0.9. The capture cross-sections of the ^{99}Tc, ^{129}I and ^{135}Cs isotopes are higher in low energy region (<1keV) with respect to in high energy region. Therefore, the volume fraction of graphite is raised from 10 to 80% stepped by 5% to slow down the energy of neutrons entering into the TZ_{FP} while the VF_{FP} is reduced from 80 to 10% depending on the graphite volume fraction. Thus the slowed down neutrons would be more efficiently utilized for transmuting the LLFPs. The material compositions and dimensions of all zones that constitute the blanket are given in Table 2.

Table 2. The material compositions and dimensions of the zones of the improved blanket

Zone	Material	Dimension [cm]	Fraction [%]
Cavity	Vacuum	100	
FW	C/C composite (1.85)*	3	100
	MA		from 10 to 20
TZ_{MA}	C/C composite	10	10
	[a]He (0.00715)		from 80 to 70
NMZ	Be (1.85)	1	100
TBZ	Li_2O (2.013)	12	100
RZ	Graphite (2.1)	5	100
	LLFP		from 80 to 10
TZ_{FP}	Graphite	10	from 10 to 80
	He		10
RZ	Graphite	40	100
SZ	B_4C (2.54)	5	100

* Density in g/cm^3, [a] at 40 atm.

3. CALCULATION METHOD

3.1. Calculational procedure

The neutronic calculations per D–T fusion neutron have been performed for a cylindrical one-dimensional geometry by solving the Boltzmann transport equation with the help of the neutron transport code XSDRNPM/SCALE4.4a [28] and the 238 energy groups (148 fast and 90 thermal groups) neutron transport and activity cross-section data library [29]. This library is also known as the Library to Analyze Radioactive Waste (LAW) Library. The numerical output of the XSDRNPM calculations is further processed by using the XSCALC interface code [30] to estimate neutronic parameters and transmutation characteristics per D-T fusion neutron. The calculations of the time dependent atomic densities of the isotopes have been performed for an operation period (OP) of up to 10 years by 75% plant factor (η) under a neutron wall load (P) of 5 MW/m^2.

4. NUMERICAL RESULTS

4.1. Transmutation Reactions

Two transmutation reactions are important for the nuclear waste management: (1) neutron capture and (2) fission. The aim of the nuclear waste incineration is to transmute a long-lived nuclear waste isotope to a nuclear species that is either stable or has a half-life that is much shorter than that of the original waste isotope itself. For the MAs, the fission process is a very effective way of incineration. When the MAs are irradiated by neutrons, they may either fission or capture a neutron to transmute into a higher isotope. Fission transmutation reactions will produce mostly short-lived fission products that decay into stable elements, and contribute to the neutron flux while destroying the actinides. For the LLFPs, the neutron capture transmutes them to stable or short-lived isotopes that then decay into stable isotopes.

4.2. Calculation of the pertinent physical parameters

In a hybrid reactor, the nuclides densities of the nuclear fuel vary in the blanket depending on time (t) due to the B/T (burned and/or transmuted) of them. Therefore, in order to evaluate some physical parameters of the blanket, these time dependent atomic densities must be calculated. The time dependent atomic density of nuclide i at t+Δt can be calculated as follows:

$$N_i(t+\Delta t) = N_i(t) + \Delta N_i \qquad (1)$$

where N(t) is the atomic density of the relevant nuclide at t, and ΔN_i is the net quantity of B/T densities and produced densities from the mother nuclide of the relevant nuclide during a period of Δt, and can be computed by the equations below:

$$N_{x,i} = \Phi \cdot \Delta t \cdot \int_E N_i \cdot \sigma_{x,i}(E) \cdot \phi(E) \cdot dE \qquad (2)$$

where $N_{x,i}$ is the B/T density of the relevant nuclide (daughter, i, or mother, j) by x reaction, representing one of the reactions of a (absorption), c (capture) and f (fission), during a period of Δt, $\sigma_{x,i}$ is the relevant microscopic cross-section of the relevant nuclide, ϕ is the neutron flux, and Φ is the number of fusion neutron per second, reaching to the FW, and

$$\Phi = \eta \cdot \frac{P \cdot 4.444 \cdot 10^{13}}{1 \cdot MW/m^2} \cdot A_{fw} \qquad (3)$$

where A_{fw} is the area of the FW.

$$\Delta N_i = N_{a,j} \cdot \alpha_{j \to i} + N_j(t) \cdot \lambda_j \cdot \Delta t \cdot \beta_{j \to i} - N_{a,i} - N_i(t) \cdot \lambda_i \cdot \Delta t \quad (4)$$

where $\alpha_{j \to i}$ is the probability of (n,γ) or (n,2n) reaction of nuclide j to nuclide i, $\beta_{j \to i}$ is the yield fraction for the production of nuclide i from nuclide j, and λ is the decay constant of the relevant nuclide.

The transmutation fraction (TF) is the ratio of the net B/T atomic density of a nuclide during the OP to its atomic density at the beginning of operation period (BOP),

$$TF_i = \frac{N_i(0) - N_i(T)}{N_i(0)} \quad (5)$$

Figure 2 shows the variations of the TFs of the MAs with the MA volume fraction.

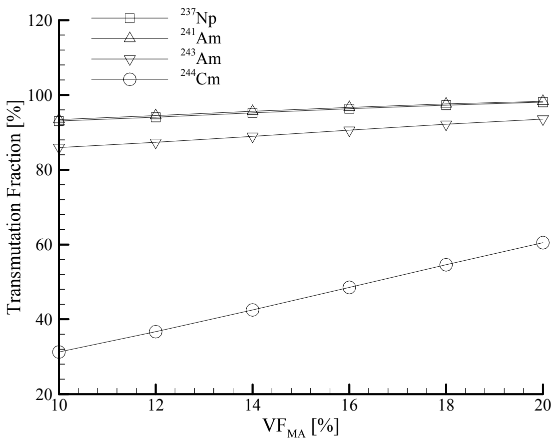

Figure 2. Variations of the transmutation fractions of the MAs with the MA volume fraction

The TFs of the MAs increase quasi-linearly depending on the MA volume fraction. The TFs of ^{237}Np and ^{241}Am have almost similar value and their TFs increase from 92 to 99%. The TFs of ^{243}Am and ^{244}Cm increase from 84 and 31% to 93 and 60%, respectively, with the increase of VF_{MA} from 10 to 20%.

The variations of the TFs of LLFPs with the MA and LLFP volume fractions are plotted in Figure 3-5. As the VF_{FP} increases from 10 to 80%, in the case of VF_{MA}= 10%, the TFs of ^{99}Tc, ^{129}I and ^{135}Cs decrease from 44.1, 36.4 and 35.5 to 8.7, 6.6 and 4.5, respectively. In the case of VF_{MA}= 20%, these decreases are from 67.7, 56.8 and 54.7 to 13.3, 10.3 and 7.0, respectively. The ^{99}Tc among the LLFP nuclides has the highest transmutation fraction.

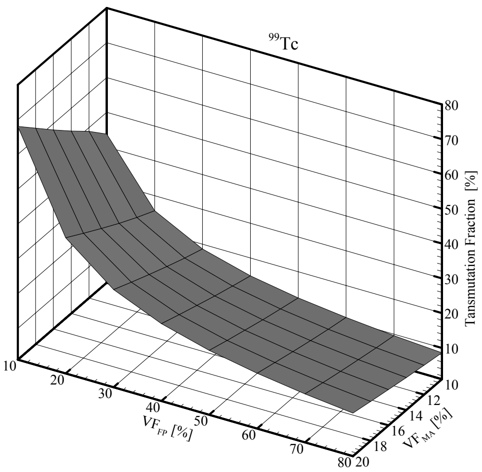

Figure 3. Variation of the transmutation fraction of ^{99}Tc with the MA and LLFP volume fractions

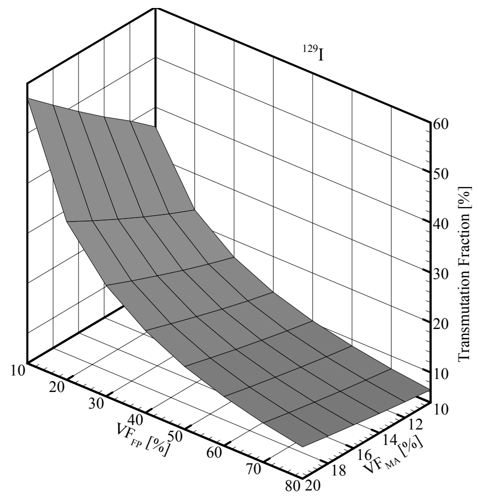

Figure 4. Variation of the transmutation fraction of ^{129}I with the MA and LLFP volume fractions

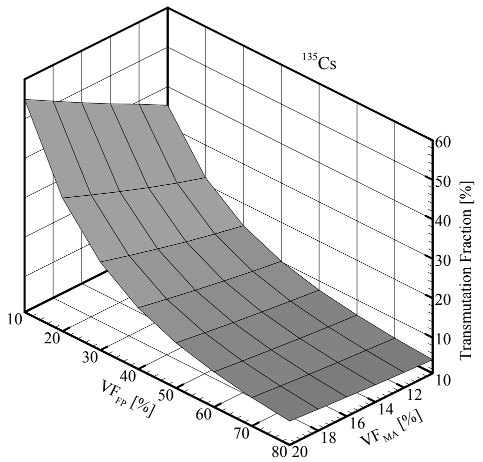

Figure 5. Variation of the transmutation fraction of ^{135}Cs with the MA and LLFP volume fractions

The effective half-life of a nuclide exposed to neutron flux can be defined as follows:

$$T_{1/2,i}^{eff} = \frac{\ln(2)}{\lambda_i^{eff}} \tag{6}$$

where λ_i^{eff} is the effective decay constant of the relevant nuclide, and

$$\lambda_i^{eff} = \lambda_i + \phi \cdot \sigma_{a,i} \text{ or } \lambda_i^{eff} = \frac{1}{T} \cdot \ln\left[\frac{N_i(0)}{N_i(t)}\right] \tag{7}$$

Substituting by Eq. (8) into Eq. (7), we get

$$T_{1/2,i}^{eff} = \frac{T \cdot \ln(2)}{\ln\left[\frac{N_i(0)}{N_i(T)}\right]} \tag{8}$$

Figure 6 shows the variations of the effective half lives of the MAs with the MA volume fraction.

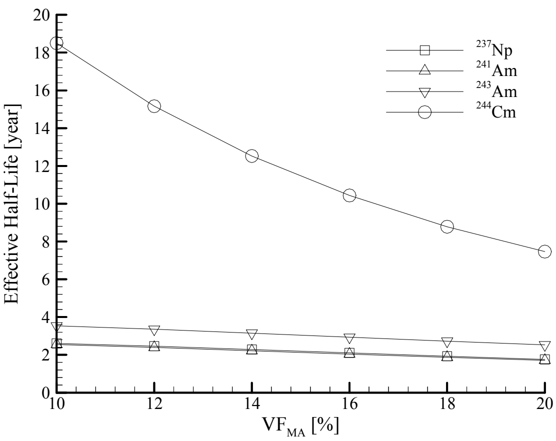

Figure 6. Variations of the effective half lives of the MAs with the MA volume fraction

As is known, the B/T of TRU nuclides in a fusion breeder reactor shortens their very long half-lives. The effective half-lives of the ^{237}Np, ^{243}Am and ^{244}Cm nuclides, therefore, also decrease from about 2.7, 3.6 and 18.4 years to 1.7, 2.5 and 7.4 years respectively. The ^{237}Np and ^{241}Am nuclides have almost similar effective half-life values. These results bring out that the rise of MA fraction (from 10% to 20%) decreases the effective half-lives.

The variations of the effective half lives of ^{99}Tc, ^{129}I and ^{135}Cs with the MA and LLFP volume fractions are plotted in Figure 7-9.

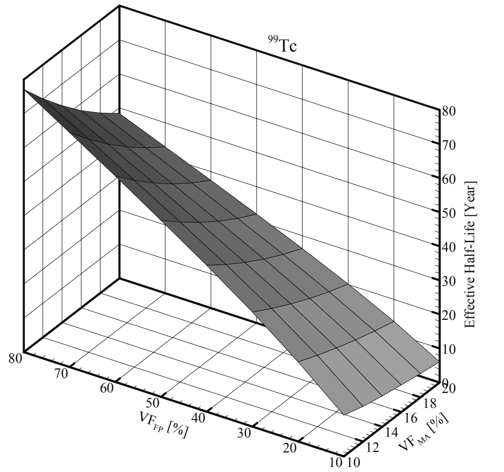

Figure 7. Variation of the effective half life of ^{99}Tc with the MA and LLFP volume fractions

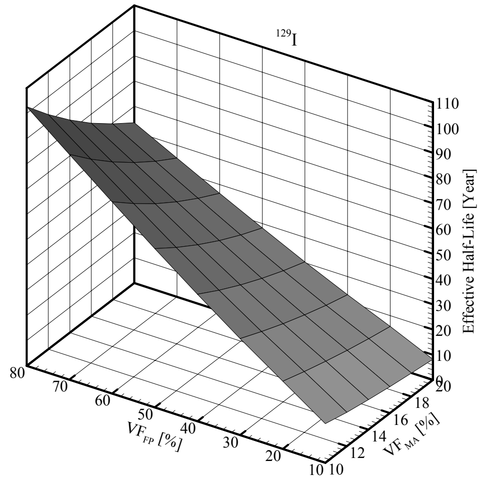

Figure 8. Variation of the effective half life of ^{129}I with the MA and LLFP volume fractions

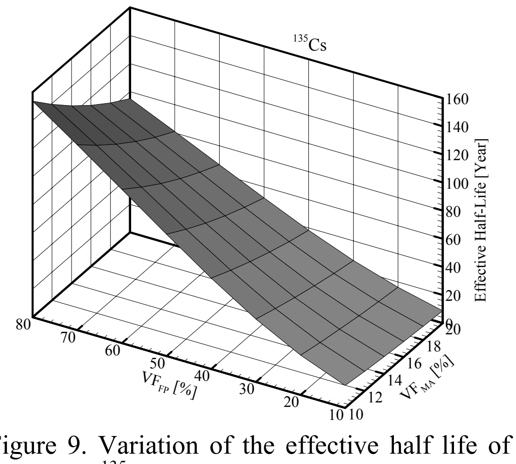

Figure 9. Variation of the effective half life of ^{135}Cs with the MA and LLFP volume fractions

The effective half lives of LLFPs increase quasi-linearly as the VF_{FP} increases from 10 to 80% and these values decrease as the VF_{MA}

increases from 10 to 20%. As the VF_{FP} increases from 10 to 80%, in the case of VF_{MA}= 10%, the effective half lives of ^{99}Tc, ^{129}I and ^{135}Cs increase from 11.9, 15.4 and 15.8 to 76.7, 102.1 and 152.7, respectively. In the case of VF_{MA}= 20%, these increases are from 6.2, 8.3 and 8.8 to 48.6, 63.8 and 95.4, respectively.

4.3. Neutronic performance of the blanket

The blanket energy multiplication factor (M) is one of the main parameters in a fusion-driven reactor, is defined as the ratio of the total amount of nuclear energy release in the blanket to the incident fusion neutron energy. It can be calculated by:

$$M = \frac{R_F \cdot E_f + 4.784 \cdot T_6 - 2.467 \cdot T_7 + 14.1}{14.1} \qquad (9)$$

where E_f is the energy per fission (200 MeV), T_6 and T_7 are the tritium breedings obtained by $^6Li(n,\alpha)T$ and $^7Li(n,n',\alpha)T$ reactions per fusion neutron, respectively. The M that is proportional with fission rate increases from 6.3 to 17.3 with the increase of VF_{MA} from 10 to 20% because of the fission reactions of the MAs in the blanket. It is shown that the FDT can produce substantial electricity in *situ*.

The peak-to-average fission power density ratio (Γ) is a measure of spatial non-uniform fission energy density that must be reduced to 1.0 for obtaining a flat fission power density. This ratio can be calculated as follows:

$$\Gamma = \frac{(R_F D)_{max}}{R_F / V_{MA}} \qquad (10)$$

The Γ varies in the range of 1.06–1.08 depending on the VF_{MA}. These values show that the fission power density profiles are very close to a uniform profile.Other important neutronic data per fusion neutron in overall blanket are given in Table 3.

Table 3. Neutronic data per D-T fusion neutron in the overall blanket (VF_{FP} =10%)

VF_{MA} [%]	10	12	14	16	18	20
M	6.3	7.9	9.7	11.8	14.3	17.3
Γ	1.080	1.070	1.068	1.065	1.067	1.064

VF_{FP} = the volume fractions of FP
VF_{MA} = the volume fractions of MA
M = the energy multiplication ratio
Γ = the peak-to-average fission power density ratio

5. CONCLUSIONS

The transmutations of both the MAs and the LLFPs in a FDT and the effects of the MA and LLFP volume fractions on these transmutations were investigated. The main conclusions derived from this study are cited briefly below:

- The transmutation fractions of the MAs increase quasi-linearly depending on the MA volume fraction.
- The transmutation fractions of LLFPs decrease quasi-linearly with the increase of VF_{FP} and these values increase with the increase of VF_{MA}. The ^{99}Tc among the LLFP nuclides has the highest transmutation fraction.
- The rise of MA fraction (from 10% to 20%) decreases the effective half-lives of the MAs.
- The effective half lives of LLFPs increase quasi-linearly with the increase of VF_{FP} and these values decrease with the increase of VF_{MA}.
- In all volume fraction cases, the blanket can provide enough tritium for its own fusion driver.

Consequently, the optimized FDT has high neutronic performance and carry out the MA and LLFP nuclides transmutation effectively while it can produce substantial electricity in *situ*.

REFERENCES

1. Übeyli M. Transmutation of minor actinides discharged from LMFBR spent fuel in a high power density fusion reactor. Energy Conversion and Management 2004;45:3219-3238.
2. Azizov E.A. et al., The concept of the volumetric neutron source on the basis of the JUST-T tokamak for minor actinides transmutation. Plasma Devices and Operations 2003;11:279-286.
3. Serikov A. et al., Possibility of fusion power reactor to transmute minor actinides of spent nuclear fuel. Fusion Engineering and Design 2002;63:93-99.
4. Feng K.M. et al., Transmutation of minor actinides in a spherical torus tokamak fusion reactor, FDTR. Fusion Engineering and Design 2002;63:127-132.

5. Feng K.M, Hu G. Transmutation of nuclear wastes in a fusion breeder. Fusion Engineering and Design 1998;41:449-454.
6. Cheng E.T, Cerbone R.J. Prospect of nuclear waste transmutation and power production in fusion reactors. Fusion Technology 1996;30:1654-1658.
7. Feng K.M, Zhang G.S. Transmutation of transuranic actinides in a spherical torus tokamak fusion reactor. Nuclear Fusion 2003;43:756-760.
8. Stankovsky A. et al., Transmutation of long-lived fission products driven by D-T and D-D fusion: Specific neutronics and radiological consequences. Fusion Science and Technology 2003;43:569-579.
9. Saito M. et al., Fusion-driven transmutation of fission product cesium in its elemental form. Journal of Nuclear Science and Technology 2000;37:1024-1031.
10. Saito M. et al., Transmutation of elemental cesium by a fusion neutron source. Nuclear Technology 2001;133:229-241.
11. Takibaev et al., Transmutation of zirconium-93 in high-flux blanket of fusion neutron source. Journal of Nuclear Science and Technology 2000;37:870-876.
12. Tsutsui H. et al., Transmutation of fission products by high-field tokamak reactor with force-balanced coils. Fusion Engineering and Design 1998;41:431-436.
13. Vasiliev N.N. et al., Burning of minor actinides and fission products from spent nuclear fuel of power plants in dual-purpose fusion reactor. Plasma Devices and Operations 2003;11:123-129.
14. Gohar Y. Fusion solution to dispose of spent nuclear fuel, transuranic elements, and highly enriched uranium. Fusion Engineering and Design 2001;58:1097-1101.
15. Stacey W.M, Hoffman E.A. Tokamak transmutation facility studies. Fusion Technology 2001;39:525-529.
16. Gohar Y. Flibe blanket concept for transmuting transuranic elements and long lived fission products. Fusion Technology 2001;39:535-540.
17. Chen Y.X, Wu Y.C. Conceptual study on high performance blanket in a spherical tokamak fusion-driven transmitter. Fusion Engineering and Design 2000;49:507-512.
18. Qiu L.J. et al., A low aspect ratio tokamak transmutation system. Nuclear Fusion 2000;40:629-633.
19. Qiu L.J. et al., Conceptual desıgn of a fusıon-fıssıon hybrıd reactor for transmutatıon of hıgh-level nuclear waste. Fusion Engineering and Design 1994;25: 167-177.
20. Yapıcı H. et al., Minor actinide transmutation potential of modified PROMETHEUS fusion reactor. Journal of Fusion Energy 2004;23:121-135.
21. Yapıcı H, Übeyli M. Power flattening in Prometheus breeder reactor using nuclear fuel and waste actinide. Annals of Nuclear Energy 2003;30:159–173.
22. Yapıcı H. Burning and/or transmutation of transuraniums discharged from PWR-UO_2 spent fuel and power flattening along the operation period in the force free helical reactor. Energy Conversion and Management 2003;44:2893-2913.
23. Yapıcı H. Determination of the optimal plutonium fraction in transuranium discharged from pressured water reactor (PWR) spent fuel for a flat fission power generation in the force-free helical reactor (FFHR) along the transmutation period. Annals of Nuclear Energy 2003;30:633-649.
24. Yapıcı H. Study on transmutation of minor actinides discharged from high burn-up PWR-MOX spent fuel in the force-free helical reactor. Annals of Nuclear Energy 2003;30:413-436.
25. Yapıcı H. Study of fissile fuel breeding concept for the force-free helical reactor. Fusion Engineering and Design 2003;65:599-609.
26. Yapıcı H, Demir N, Genç G. Neutronic Analysis for Transmutation of Minor Actinides and Long-Lived Fission Products in a Fusion-Driven Transmuter (FDT). Journal of Fusion Energy 2006; 25:225-239.
27. NEA, Calculations of Different Transmutation Concepts an International Benchmark Exercise, Nuclear Science Committee ,2000.
28. Greene N.M, Petrie L.M. XSDRNPM: A One-Dimensional Discrete-Ordinates Code for Transport Analysis, Sect. F3 of SCALE: A Modular Code System for Performing Standardized Computer

Analyses for Licensing Evaluation, NUREG/CR-0200, Rev. 6 (ORNL/NUREG/CSD-2/V2/R6), Vols. I, II, and III. Version 4.4a of the code package is available from Radiation Safety Information Computational Center (RSICC) at Oak Ridge National Laboratory as CCC-545, 2000.

29. Greene N.M, Arwood J.W. RQ. Wright, CV. Parks, The LAW Library–A Multi group Cross-Section Library for Use in Radioactive Waste Analysis Calculations, ORNL/TM-12370, Martin Marietta Energy Systems, Inc., Oak Ridge Natl. Lab. 1994.

30. Yapıcı H, XSCALC for Interfacing Output of XSDRN to Calculate Integral Neutronic Data, Erciyes University/TURKEY, 2001.

Nomenclature

Abbreviation

B/T burning and/or transmutation
CR conversion ratio
D-T deuterium-tritium
EC electron capture
FDT fusion-driven transmuter
FFHR force-free helical reactor
FW first wall
HLW high-level waste
LLFP long-lived fission product
MA minor actinide
MOX mixed oxide
NMZ neutron multiplier zone
PWR pressured water reactor
RZ reflector zone
SZ shielding zone
TBR tritium breeding ratio
TBZ tritium breeding zone
TRU transuranium
TZ transmutation zone
VF volume fraction in percentage

Subscript

FP long-lived fission product
MA minor actinide